



Load optimization on the performance of combined cycle power plant Block 4 PT Indonesia Power Priok POMU

Louise Indah Utami^{a,*}, Ika Yuliyani^a, Yanti Suprianti^a, Purwinda Iriani^{a,b}

^a Energy Conversion Engineering Department, Bandung State Polytechnic
Gegerkalong Hilir Road, West Bandung, 40559, Indonesia

^b Chemistry Department, University of Warwick
Coventry CV4 7AL, United Kingdom

Received 12 November 2021; Revised 29 November 2021; Accepted 8 December 2021; Published online 29 July 2022

Abstract

Combined cycle power plant (CCPP) is a closed-cycle power plant, where the heat from the gas turbine's (GT) exhaust gas will be streamed to the heat recovery steam generator (HRSG) to be utilized by steam turbine (ST). CCPP Block 4 (Jawa-2) PT Indonesia Power Priok POMU has an installed capacity of 880 MW, consists of 2 GT units (301.5 MW each) and 1 ST unit (307.5 MW). The performance of a power plant depends on its load, as the efficiency of the turbine generator is low when operated at low loads. The data as of July 2019 showed that 2.2.1 (2 GT, 2 HRSG, 1 ST) configuration has been used in three conditions where the CC net load was around 30 - 45 %, which in fact could be compensated by the 1.1.1 (1 GT, 1 HRSG, 1 ST) configuration. This resulted in a decrease of the CC net efficiency up to 21.34 %. The optimization that can be done is to change the load configuration from 2.2.1 to 1.1.1 at 0 - 50 % of CC net load through simulations, by including the influence of the GT and HRSG start-up processes. The result of this optimization is that the CCPP performance increases due to higher performance of each turbine generator. Thus, the optimization results during July 2019 provided energy saving of 1,146.09 MMBTU or equivalent to cost saving of IDR 152,249,551.76.

Copyright ©2022 National Research and Innovation Agency. This is an open access article under the CC BY-NC-SA license (<https://creativecommons.org/licenses/by-nc-sa/4.0/>).

Keywords: combined cycle; gas turbine; steam turbine; load optimization; power plant performance.

I. Introduction

PT Indonesia Power Priok Power Generation and O&M Unit (POMU) manages four CCPP Blocks with a total installed capacity of 2,800 MW. The CCPP Block 4 (Jawa-2) is the newest generating unit in the Priok POMU, which has been operating (open cycle) since June 2018 and completed the integration with its ST unit (combined cycle) in May 2019. CCPP Block 4 is connected to the Jawa-Bali power system, with an installed capacity of 880 MW and consists of 2 GT units and 1 ST unit.

The power plant performance parameters include efficiency and heat rate, which are closely related to its load [1][2][3]. When the turbine generator load is well below its design capacity, its efficiency will also drop significantly. Therefore, it is important to keep the turbine generator loaded according to its capacity; especially at low

generation loads. In the manual book, the 2.2.1 configuration is used when the CC net load is more than 45 %. Meanwhile, several conditions at the site (July 2019) showed that the 2.2.1 (2 GT, 2 HRSG, 1 ST) configuration has been used in the CC net load of around 30 - 45 %, resulted up to 21.34 % reduction in the efficiency of the generating unit. The lower efficiency is certainly detrimental because more fuel is needed for the same generated power [4][5].

Because the CC load varies over time, the effort that can be made is to set each turbine generator load to remain high [6][7][8]. The setting is done by distributing the turbine generator load at the right part load [9][10], so that the CC performance remains high wherever the load is.

This journal will discuss optimization in the form of changing the loading configuration from 2.2.1 (2 on 1) to 1.1.1 (1 on 1) at 0 - 50 % of CC net load by including the influence of the GT and HRSG start-up processes, and show the actual part load efficiency which actually occurs in real conditions.

* Corresponding Author. Phone: +62-222011095
E-mail address: louiseindahutami@gmail.com

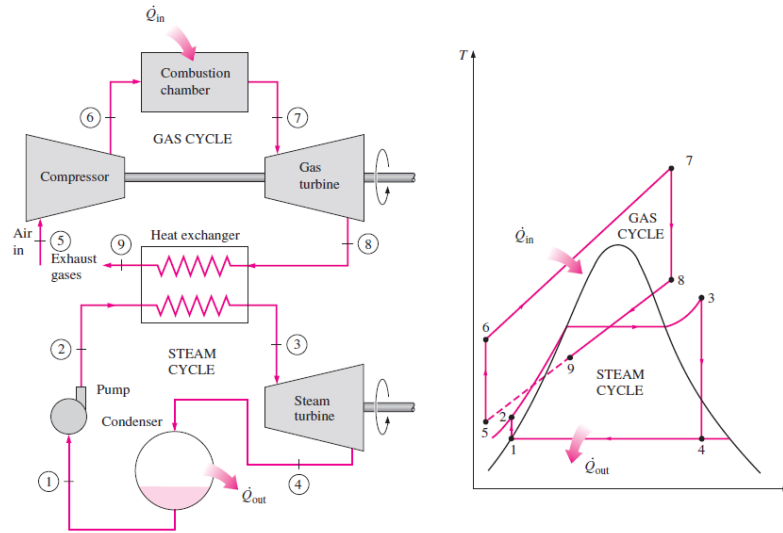


Figure 1. Flow diagram and T-s diagram of CCPP [12]

II. Materials and Methods

A. Combined cycle power plant (CCPP)

Simple cycle gas turbine and combined cycle gas turbine power plants have traditionally served as peaking units because they can be started within minutes and ramped up and down quickly to meet spikes in demand or sudden changes in electric system loads. Combined cycle power plants can respond to load changes faster than conventional steam power plants [11].

The term of combined cycle (CC) refers to the combining of multiple thermodynamic cycles to generate power [11], as shown in Figure 1. The first cycle is the Brayton cycle which consists of a compressor, combustion chamber, and the gas turbine (GT) itself. The second cycle is the Rankine cycle which consists of pumps, heat recovery steam generator (HRSG), the steam turbine (ST), and a condenser.

Brayton cycle occurs at high temperature and the Rankine cycle occurs with lower temperature. While conventional thermal plants discard waste gases to the environment at high temperature, combined cycle plants take advantage of these gases at high temperatures. The exhaust heat from the gas turbine cycle is used to generate steam at high pressure and high temperature that will be expanded in a steam turbine to generate additional power [13].

In this cycle, energy is recovered from the exhaust gases by transferring it to the steam in a

heat exchanger that serves as the boiler. In general, more than one gas turbine is needed to supply sufficient heat to the steam. Also, the steam cycle may involve regeneration as well as reheating. Energy for the reheating process can be supplied by burning some additional fuel in the oxygen-rich exhaust gases [12].

In comparison with steam power plants which offer a thermal efficiency of about 40 %, combined cycle power plants deliver a thermal efficiency of about 60 % (based on lower heating values) [14].

B. CCPP working principle

The CCPP layout is shown in Figure 2. The gas turbine of CCPP is maneuverable and can change output power faster than steam turbine. Steam turbine in CCPP operates under variable pressure. So, steam turbine power varies with long response time depending on gas turbine power [15].

After passing the compressor, air is mixed with fuel in combustion chamber. The mixture burns and hot gases are expanded in gas turbine then rotate it. After the gas turbine, hot gas goes to HRSG, where it heats water. Water becomes a steam which rotates the steam turbine [15].

C. CCPP performance

1) Gas turbine (GT) heat rate and efficiency

$$GTiHR = \frac{F_{fuel} \times LHV_{fuel}}{P_{GTiG} \times 1000 \times 4.184} \tag{1}$$

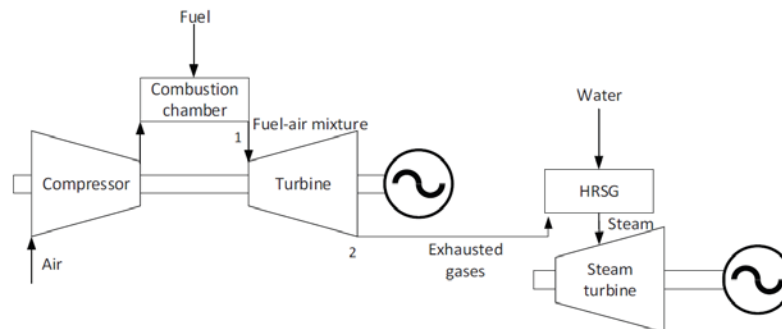


Figure 2. CCPP layout [15]

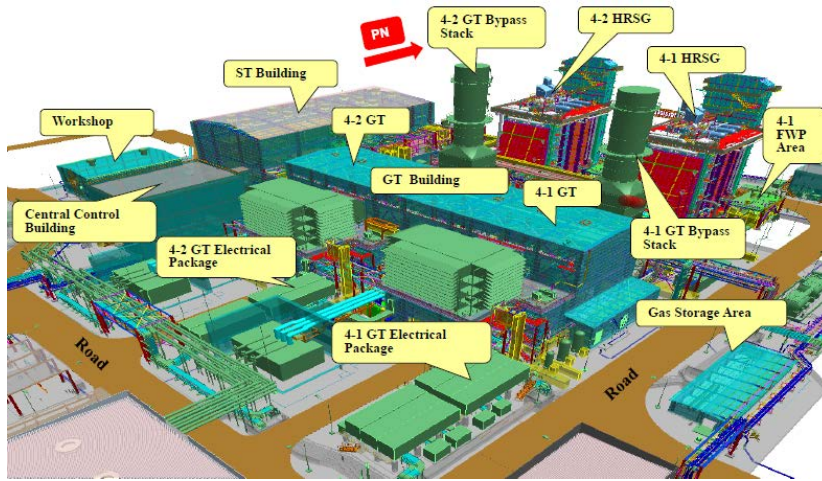


Figure 3. CCPP Block 4 Priok POMU

$$\eta_{GTi} = \frac{860}{GTiHR} \times 100\% \quad (2)$$

$$i = 1 \sim 2, i = 1 \rightarrow GT1, i = 2 \rightarrow GT2 \quad (3)$$

where $GTiHR$ is GT heat rate, F_{fuel} is fuel flowrate, LHV_{fuel} is fuel LHV, P_{GTiG} is active power GTG, and η_{GTi} is GT efficiency.

2) Steam turbine (ST) heat rate and efficiency

$$G_{LEAK} = 1,4797 \times 10^{-8} G_{HP}^2 + 1,0555 \times 10^{-2} G_{HP} + 8,1584 \times 10^3 \quad (4)$$

$$G_{CRH} = G_{HP} - G_{LEAK} \quad (5)$$

$$G_{HRH} = G_{CRH} + G_{IP} \quad (6)$$

$$H_{ST} = (H_{HP} \times G_{HP}) + (H_{HRH} \times G_{HRH}) + (H_{LP} \times G_{LP}) - (H_{CRH} \times G_{CRH}) - (H_{CW} \times G_{GC}) \quad (7)$$

$$STHR = \frac{H_{ST}}{P_{STG} \times 4.184} \quad (8)$$

$$\eta_{ST} = \frac{860}{STHR} \times 100\% \quad (9)$$

where G_{LEAK} is turbine leakage flow, G_{HP} is HP main steam flow, G_{CRH} is cold reheat steam flow, G_{HRH} is hot reheat steam flow, G_{IP} is IP steam flow, G_{LP} is LP steam flow, G_{GC} is condenser condensate flow, H_{HP} is HP steam enthalpy, H_{CRH} is hot reheat steam enthalpy, H_{HRH} is hot reheat steam flow, H_{LP} is LP steam flow, H_{CW} is condensate enthalpy, H_{ST} is ST heat input, $STHR$ is ST heat rate, and η_{ST} is ST

efficiency.

3) Net plant heat rate and net efficiency

$$NPHR = \frac{F_{fuel} \times LHV_{fuel}}{P_{net} \times 1000 \times 4.184} \quad (10)$$

$$P_{net} = P_{net\ GT1} + P_{net\ GT2} + P_{net\ ST} \quad (11)$$

$$\eta_{NET} = \frac{860}{NPHR} \times 100\% \quad (12)$$

where $NPHR$ is net plant heat rate, F_{fuel} is fuel flowrate, LHV_{fuel} is fuel LHV, P_{net} is block net active power, and η_{NET} is net plant efficiency.

D. CCPP Block 4 Priok POMU

CCPP Block 4 (Jawa-2) Priok POMU is located in North Jakarta, with the power plant's overview shown in Figure 3. CCPP Block 4 is an asset owned by PT Perusahaan Listrik Negara and operated by PT Indonesia Power. CCPP Block 4 is the newest generating unit in Priok POMU, manufactured by Mitsubishi Hitachi power systems (MHPS). This generating unit has an installed capacity of 880 MW and has been operating since May 2019. The CCPP Block 4 consists of two gas turbines (GT), two heat recovery steam generators (HRSG), one steam turbine (ST), and one condenser as shown in Figure 4.

Table 1 shows the performance of CCPP Block 4 according to the manufacturer's design, with variations in the loading configuration of 1.1.1 (1 GT,

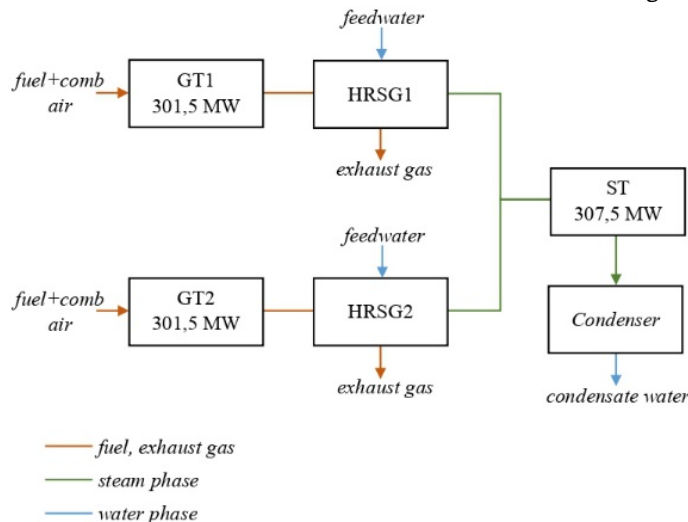


Figure 4. CCPP Block 4 Priok POMU scheme

4.1 Operational Capability

Operational Capability

Normal operation load range	: 2on1 880MW~410MW (100%~47%) 1on1 420MW~225MW
Minimum Generation load	: 2on1 400 MW (45% load) 1on1 225 MW (50% load)
Block ramp rate	
2 GTs + ST	: 44 MW/min. (410 MW* to 836MW) : 4 MW/min. (836MW* to 880 MW)
1 GT + ST	: 21 MW/min. (225 MW* to 399 MW) : 2 MW/min. (399MW* to 420 MW)
Block de-loading rate	
2 GTs + ST	: 44 MW/min. (880 MW* to 410 MW)
1 GT + ST	: 21 MW/min. (420 MW* to 225 MW)
GT ramp rate	: Max. 6.7 %(GT)/min

Figure 5. Loading configuration based on design



Figure 6. GT M701F4 rotor

1 HRSG, 1 ST) and 2.2.1 (2 GT, 2 HRSG, 1 ST). Figure 5 shows the limits for the use of 1.1.1 and 2.2.1 configurations, as well as the maximum limits for ramp-up or ramp-down rates. It is written that the 2.2.1 configuration is used when the generating load is from 410 MW to 880 MW (47 - 100 %). If the 2.2.1 configuration is used at lower loads, then the performance will be lower as well.

1) GT M701F4 (MHPS Takasago) 2 x 301.5 MW

There are two GTs (GT1 and GT2) with an installed capacity of 301.5 MW each. In Figure 6, the right side is the air compressor rotor and the left side

Table 1. CCPP Block 4 Priok POMU performance based on design

Load configuration	Parameter	Unit
1 on 1	Plant output	566 MW
	Plant efficiency	62.0 % LHV
2 on 1	Plant output	1,135 MW
	Plant efficiency	62.2 % LHV
Starting time		45 minutes

Table 2. GT M701F4 specifications

Parameter	Unit
Frequency	50 Hz
ISO base rating	385 MW
Efficiency	41.9 % LHV
LHV heat rate	8,592 kJ/kWh 8,144 BTU/kWh
Exhaust flow	748 kg/s 1,650 lb/s
Exhaust temperature	630 °C 1,167 °F
Exhaust emission	NOx 25 ppm @15 % O ₂ CO 10 ppm @15 % O ₂
Turn down load	45 %
Ramp rate	38 MW/min
Starting time	30 minutes

is the turbine rotor itself. The compressor impeller and turbine blades are in the form of airfoils and are made in stages so that the work generated from the combustion process by the combustor will be maximized. Table 2 shows the gas turbine (GT) specifications according to manufacturer's design; including efficiency and heat rate when the GT is fully loaded (100 %), as well as the allowed ramp rate limit.

2) HRSG (MHPS Kure)

There are 2 HRSG units, namely HRSG1 and HRSG2. Figure 7 shows heat recovery steam generator (HRSG) 3D design. It can be seen that the

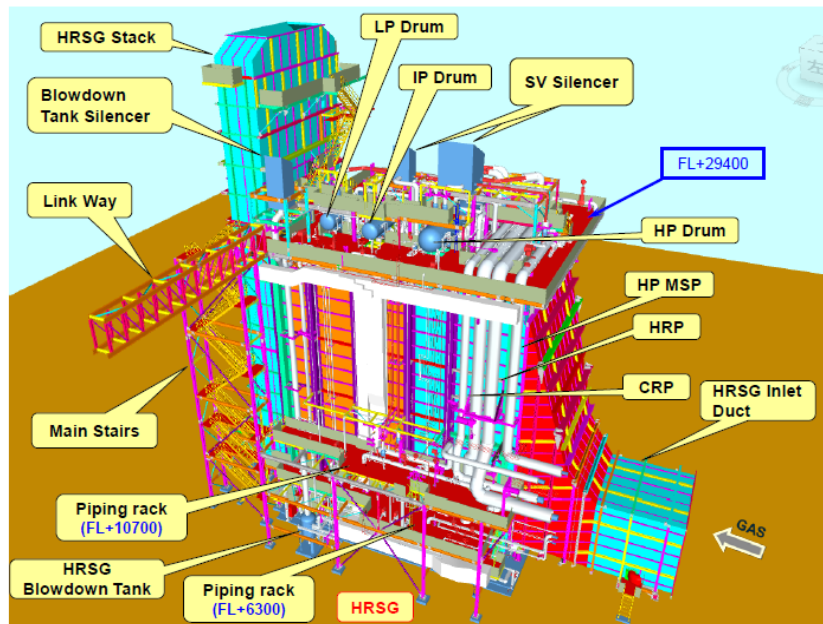


Figure 7. HRSG structure

2. HRSG Performance Design (1)

2-1. Performance Design Conditions

The heat recovery steam generator (HRSG) is triple pressure, reheat, natural circulation, horizontal gas flow type, and designed based on following conditions.

<Operating Conditions>	Design Point
Load Condition	100%LOAD
Fuel	Natural Gas
Ambient Temperature	30 °C
Ambient Pressure	101.3 kPa
Relative Humidity	83 %
Cond Inlet Temperature	30 °C
<Gas turbine exhaust gas at HRSG inlet> --- Heat Input from Gas Turbine (GT)	
Gas Flow	2502.7 t/h
Gas Temperature	606.7 °C
Gas Turbine Emissions	
O2	13.54 wt. %
N2	72.17 wt. %
Ar	1.29 wt. %
CO2	6.19 wt. %
H2O	6.81 wt. %

2. HRSG Performance Design (2)

<HRSG Performance>	
HP Steam, Superheater Outlet	
Flow	289.5 t/h
Pressure	164.1 kg/cm ² a
Temperature	581.7 °C
IP Steam, Superheater Outlet	
Flow	60.3 t/h
Pressure	39.3 kg/cm ² a
Temperature	294.2 °C
Cold Rehaet Steam, Reheater Inlet (before mixing IP Steam)	
Flow	274.4 t/h
Pressure	38.9 kg/cm ² a
Temperature	371.6 °C
Hot Rehaet Steam, Reheater Outlet	
Flow	334.7 t/h
Pressure	36.9 kg/cm ² a
Temperature	581.0 °C
LP Steam, Superheater Outlet	
Flow	51.1 t/h
Pressure	6.60 kg/cm ² a
Temperature	291.3 °C
Feedwater	
Temperature (before mixing FGH return)	39.6 °C
Temperature (LP Economizer Inlet)	55.0 °C



Figure 8. HRSG heat balance design: (a) Section 1; (b) Section 2

HP tubes are in the front side, the IP tubes are in the middle side, and the LP tubes are at the rear side of the HRSG. This causes the steam temperature at HP tubes to be the highest, while in the LP tubes is the lowest; because the heat energy from the GT exhaust gas has been absorbed by the HP and IP tubes first. Figure 8 shows the HRSG heat balance according to manufacturer's design; containing technical specifications of exhaust gas from GT, feedwater, and steam in HP, IP, CRH, HRH, and LP drums.

3) ST TC2F-40.5" (MHPS Nagasaki) 1 x 307.5 MW

There is one ST with an installed capacity of 307.5 MW. ST will reach its full load if both GT1 and

GT2 are also operated at full load (2 x 301.5 MW), because the heat utilization that can be generated by ST only reaches about 50 % of the heat in the GT exhaust gas. ST gets its steam supply from the combination of the HRSG1 and HRSG2.

As shown in Figure 9, there are three types of blades on the ST rotor, each of which operates at different pressures. The HP turbine is on the right side, followed by the IP turbine in the middle side, and the LP turbine is on the left side of the ST. Meanwhile the generator rotor is installed on the left end, with the shaft coupled with the three turbine rotors so that they all have one shaft. There are also several specifications including steam pressure and temperature in HP, IP, and LP turbines.

- Type: TC2F- 40"
- Output: 307,500 kW
- Revolution: 3,000 rpm (Clockwise viewed from Gov. side)
- HP Steam Conditions: 157.0 bara × 580.0 °C
- IP Steam Conditions: 35.4 bara × 580.0 °C
- LP Steam Conditions: 5.9 bara × 290.0 °C
- Exhaust Pressure: 706 mmHg

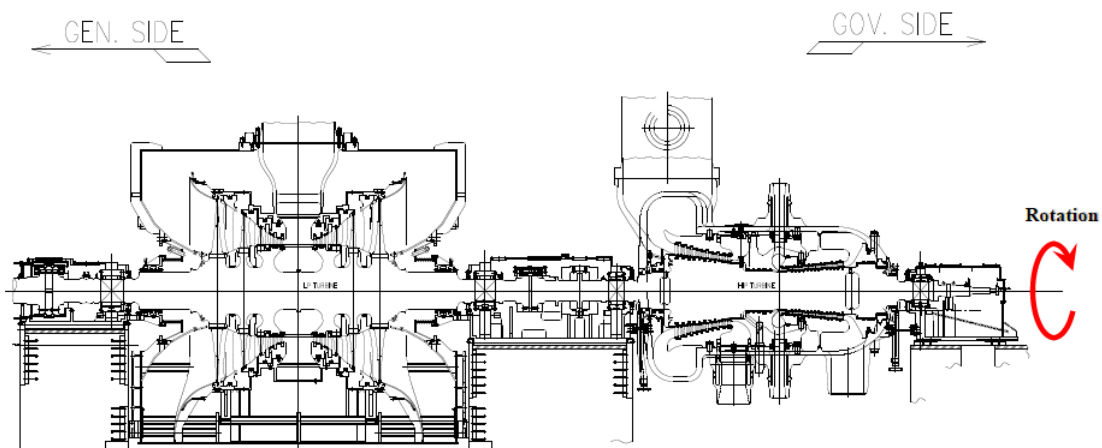


Figure 9. ST TC2F-40.5" technical specifications

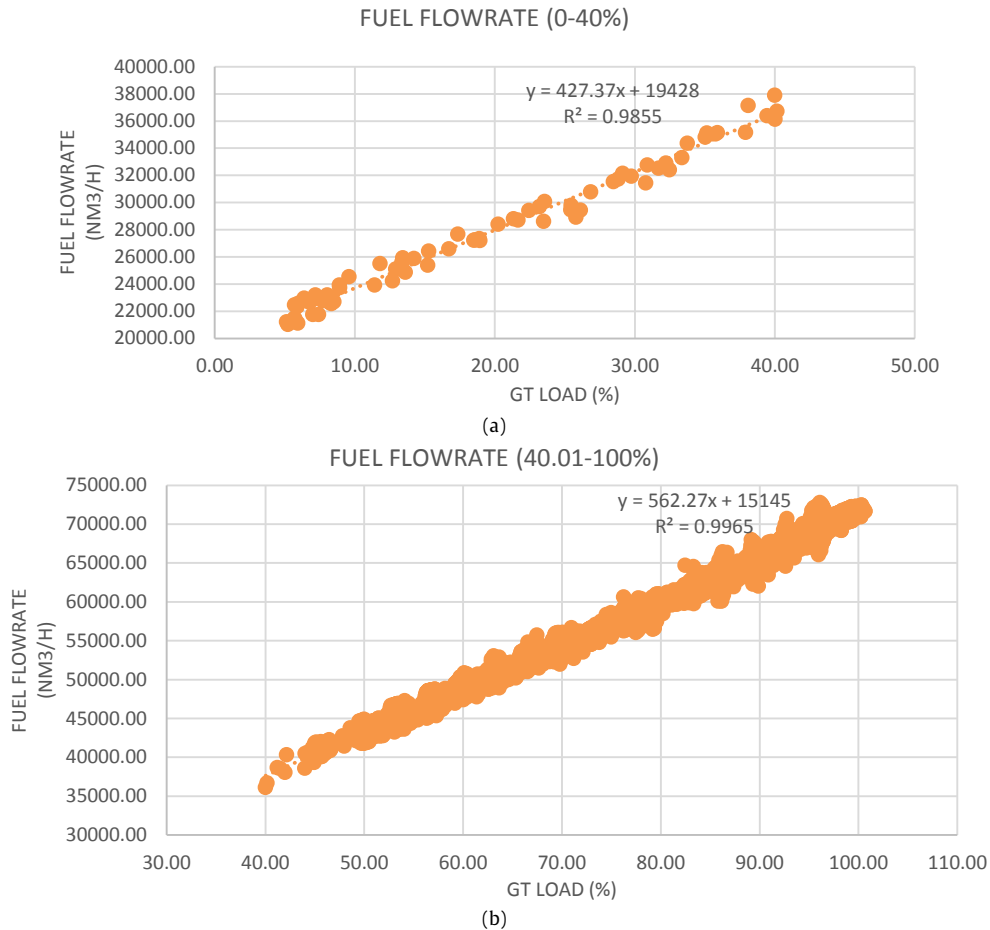


Figure 10. Fuel flowrate vs GT load: (a) 0 - 40 %; (b) 40.01 - 100 %

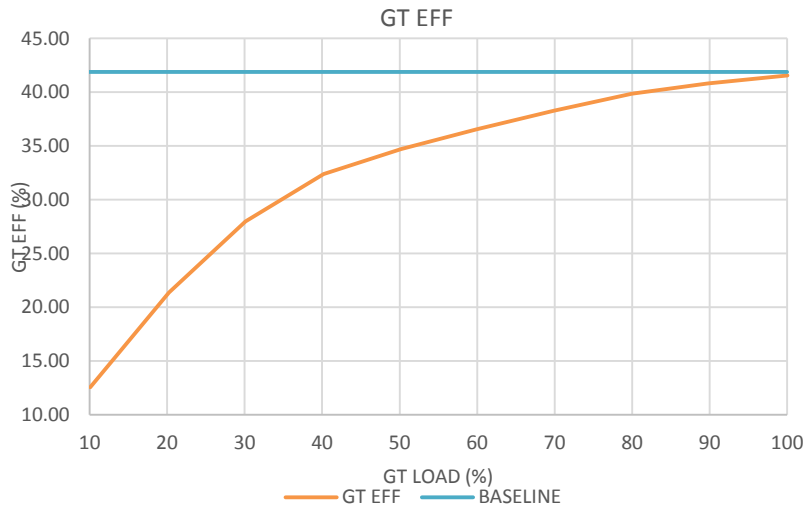


Figure 11. GT efficiency vs GT load

III. Results and Discussions

Observations were made during July 2019, with data collected by measuring instruments in one minute intervals.

A. GT analysis

Figure 10 and Figure 11 shows the relationship between GT efficiency and the GT load itself. It is seen that the efficiency is high at full load, and low when the load is also low. This happens because the

fuel required to maintain the turbine's torque remains the same when the load (electrical power) of the generator is set high or low. Therefore, the GT load must be ensured to be high in order to maintain its high performance.

B. CC analysis

Figure 12 contains two variables, namely the ratio of GT load and ST load which is a function of CC net load. The sum of the ratios of GT load to ST load will be equal to 1. For example, at 30 % of CC net load (264 MW) the ratio of GT load is 0.63 and ST

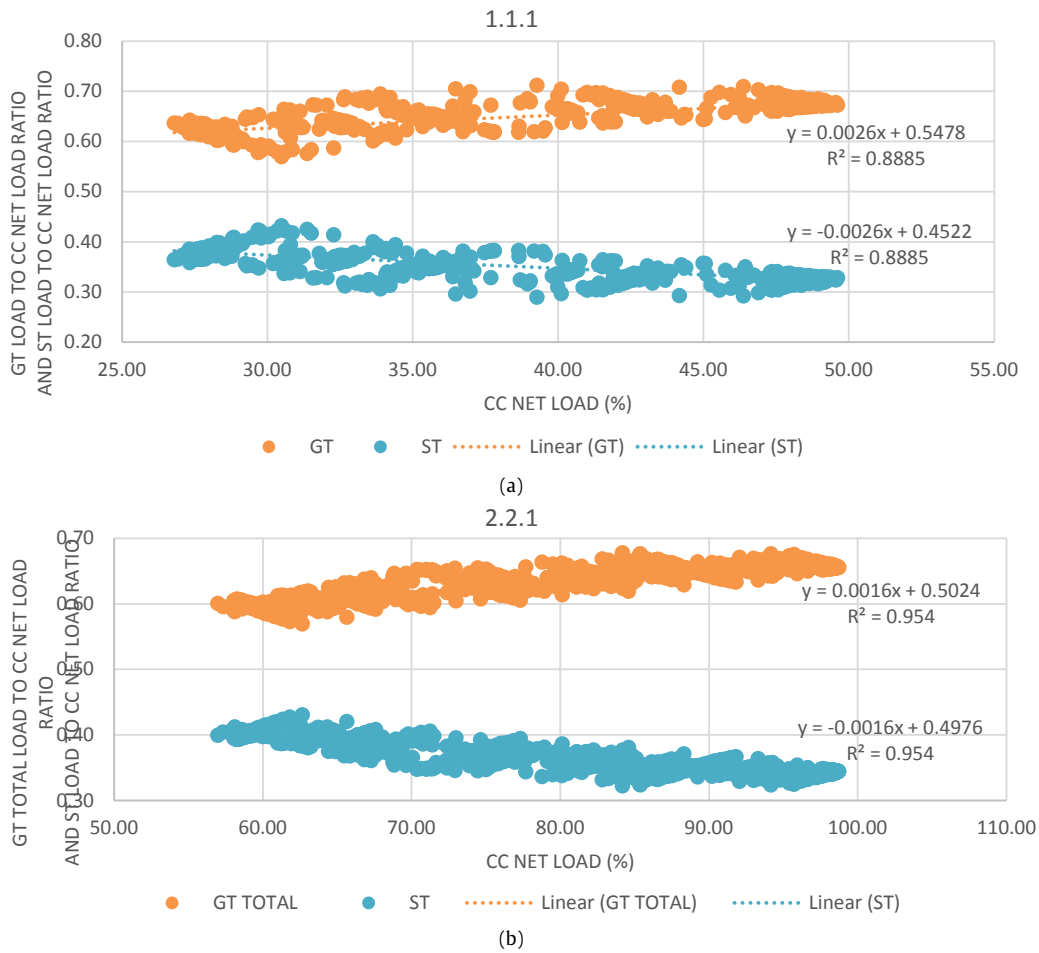


Figure 12. GT load and ST load ratio vs CC net load: (a)1.1.1 configuration; (b) 2.2.1 configuration

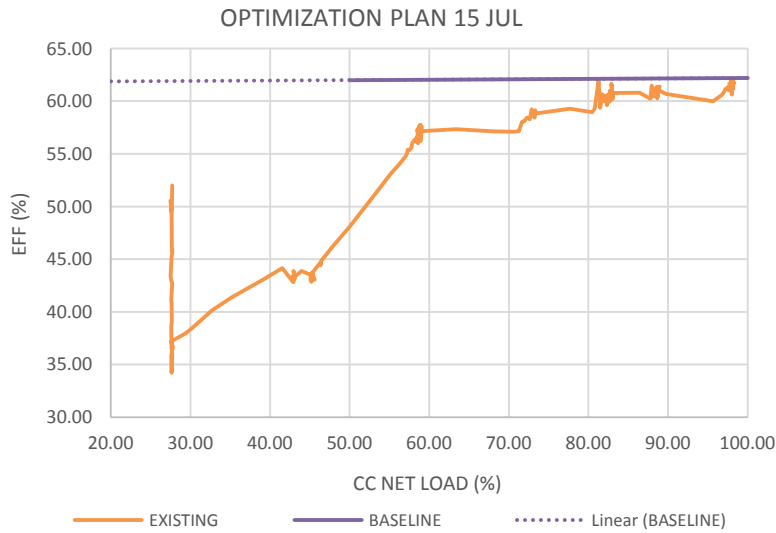


Figure 13. CC efficiency at sample existing condition

load is 0.37; this means that GT supplies 0.63 x 264 MW and ST supplies 0.37 x 264 MW. The first graph is taken at 1.1.1 configuration, while the second graph is taken at 2.2.1 configuration (includes GT and HRSG start-up processes). These equations will be used for load optimization of 1.1.1 and 2.2.1.

In Figure 13, there is a condition where the CC efficiency decreases drastically at the same load. This condition occurs when one of the GT starts up, which takes about 25 minutes. This means that during this period there is fuel consumption but the GT has not been able to produce electric power. In

addition, another consideration is the impact of GT start-up in the load of 2.2.1 on HRSG start-up processes which will be explained in the next paragraph.

As shown in Figure 14, the load configuration is 1.1.1 (GT2 on, GT1 off). When the load configuration is changed to 2.2.1 (GT1 is turned on, marked by the area in the box), it can be seen that the ST load does not increase immediately (there is a time difference of about 45 minutes since GT1 was on, or 70 minutes since GT1 started up). This is the impact of the HRSG1 start-up process, where the 45 minutes

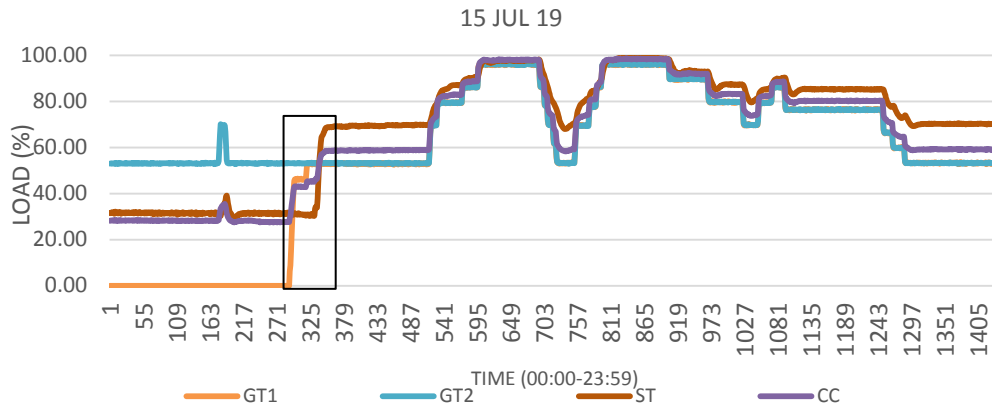
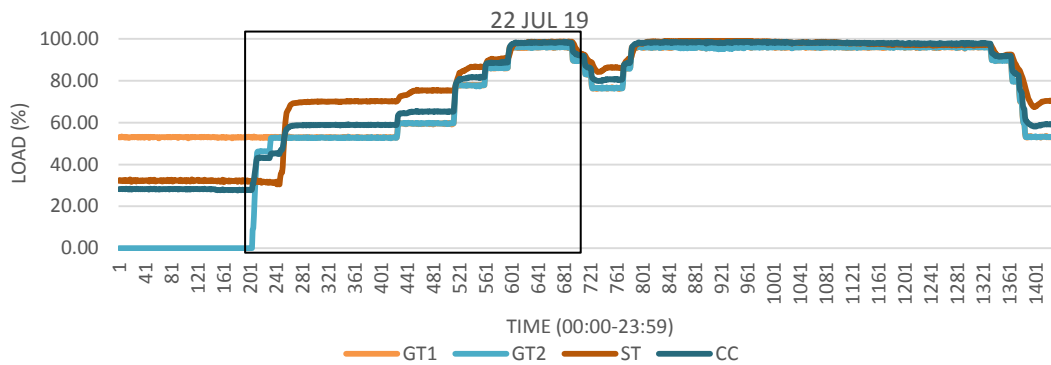
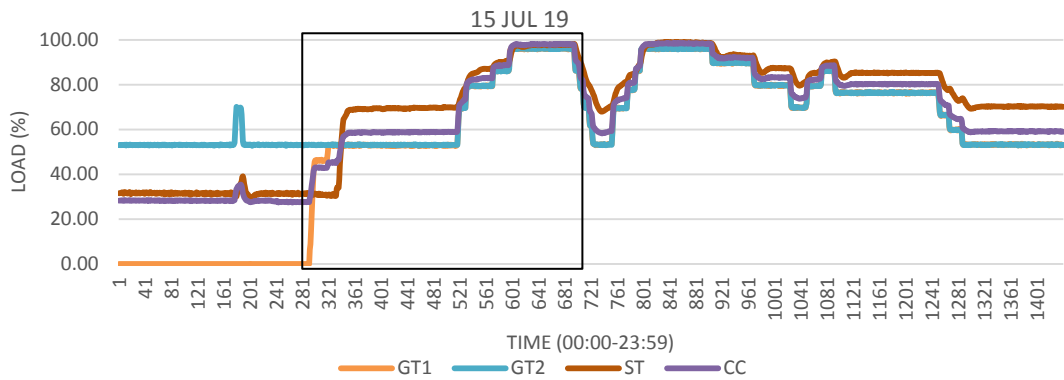
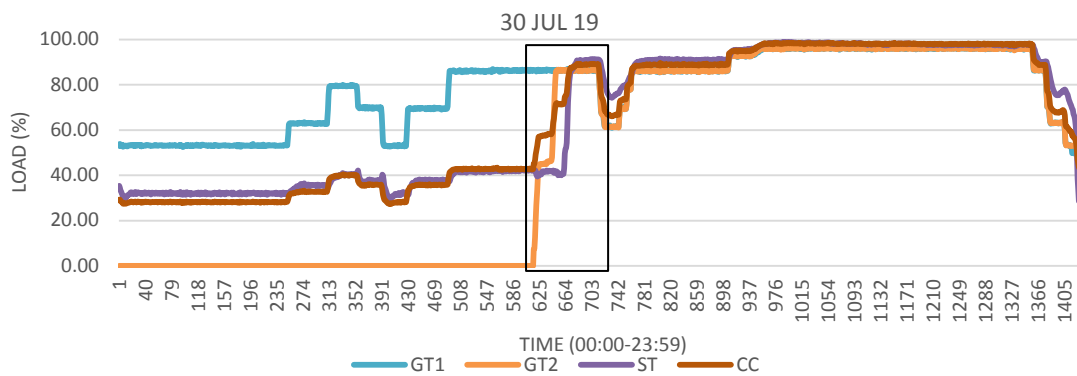


Figure 14. ST response to HRSG start up



(a)

(b)



(c)

Figure 15. Optimization data targets: (a) 15 July; (b) 22 July; (c) 30 July

difference represents the time needed for HRSG1 to produce steam before flowing it to the ST. After this time difference, HRSG1 will be able to immediately respond if there is a change in load on GT1.

C. Load monitoring

During the observations in July 2019, there were three conditions that could be optimized as shown in Figure 15. In these three conditions, the 2.2.1

Table 3.
Load optimization plan

CC net load when starting 2.2.1 (%)	HRSG start-up (mins)	Optimization	
		Start time	End time
29.43	42	15/07/2019 04:27:00	15/07/2019 11:34:00
30.57	42	22/07/2019 02:58:00	22/07/2019 11:31:00
45.13	45	30/07/2019 09:53:00	30/07/2019 11:52:00

configuration was used around 30 - 45 % of CC net load which should be compensated by the 1.1.1 configuration.

Optimization will be carried out on the three data, starting from GT start-up process and ending when the CC net load starts to decrease. The time span of the load optimization plan for the three data targets is shown in the Table 3.

D. Determination of load configuration

From the three load optimization targets, a data sample was taken; namely July 15, at 04:27 - 11:34 for optimization simulation. In the sample data, three analysis were carried out with the variables listed in the Table 4.

Figure 16 shows that the highest efficiency is achieved with option number 2, which is using the 2.2.1 configuration when the GT load has reached 100 %. Option number 2 results in better performance compared to option number 3 (according to the manual book). The baseline itself is the design efficiency according to Table 1.

The load optimization will be carried out when the configuration moves from 1.1.1 to 2.2.1, with the following conditions.

1. There is one GT which will later be referred to as the main GT, and one other GT which will later be referred to as the follower GT. The main GT is a GT which is already on at low load and will become a fully charged GT (100 %). Meanwhile, the follower GT is a GT that will be operated only when the main GT has reached full load and a higher CC net load is desired. This means when load settings occur, tuning will only be carried out on the follower GT, while the main GT will remain at full load. Meanwhile, the HRSG that is installed on the main GT will be referred to as the

Table 4.
Optimization plan options

No	Name	Description
1	Existing	2.2.1 configuration when CC net load reaches 29,58 % and above
2	Optimization plan	2.2.1 configuration GT load reaches 100% (or about 50 % CC net load)
3	Manual book	2.2.1 configuration when CC net load reaches 45 % and above

main HRSG and the HRSG that is installed on the follower GT will be referred to as the follower HRSG. The main GT and the follower GT can be GT1 and GT2, or vice versa namely GT2 and GT1. Also for the main HRSG and the follower HRSG can be HRSG1 and HRSG2, or vice versa namely HRSG2 and HRSG1.

2. In ramp-up conditions, the GT load can only be increased. Likewise in ramp-down conditions, the GT load can only be lowered. The ramp rate follows the procedure in the manual book in Figure 5, which is a maximum of 44 MW/minute.
3. In low load conditions (0 - 50 % of CC net load), the load configuration used is 1.1.1 until the main GT is fully charged (100 %).
4. In high load conditions (50 - 100% of CC net load), the load configuration used is 2.2.1 by starting up the follower GT. It takes about 25 minutes of the start-up of follower GT, and about 45 minutes (or 70 minutes from the start-up of follower GT) of the follower HRSG start-up process so that the ST load can respond to changes in the follower GT load.
5. The ramp-up process when the load configuration shifts from 1.1.1 to 2.2.1 is done by operating the main GT at full load, then proceed with tuning; namely increasing the follower GT load slowly until the desired load is reached. Meanwhile, the ramp-down shifting from 2.2.1 to 1.1.1 configuration is carried out while still operating the main GT at full load, then tuning is done by slowly lowering the follower GT load until the desired load is reached. In these two conditions (ramp-up and ramp-down), the main GT is prioritized to operate at full load.

E. Load optimization

As shown in Figure 17, the net efficiency of the CC increases after optimization, because the main GT

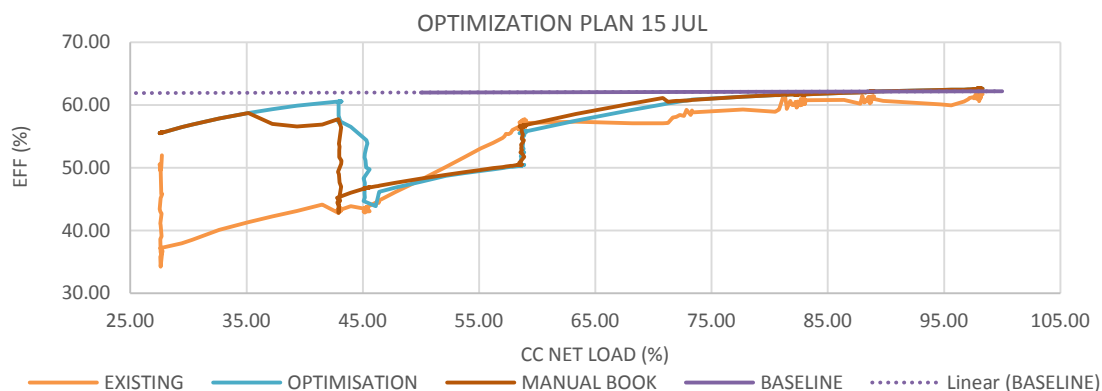


Figure 16. Optimization plan options

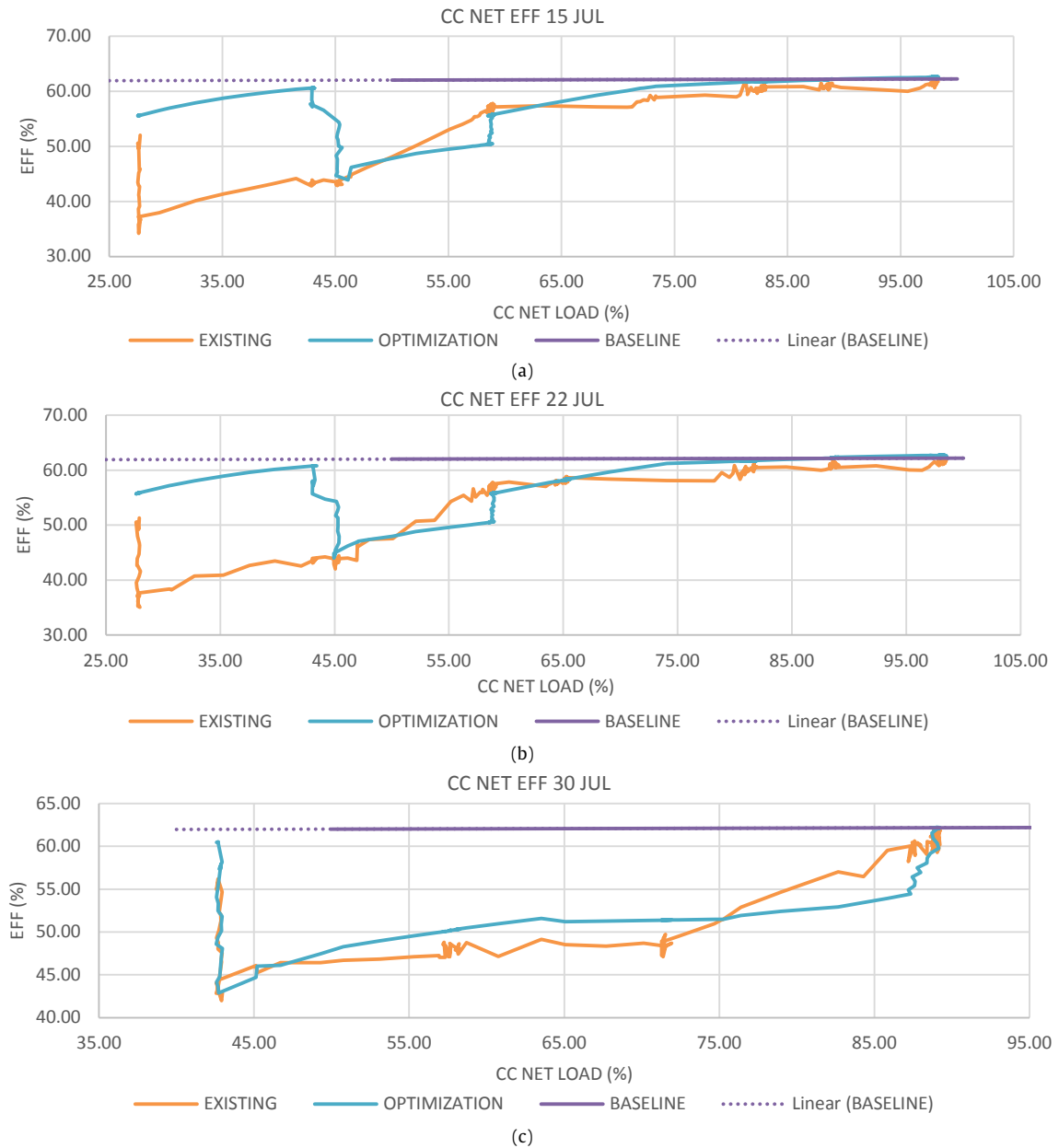


Figure 17. CC net efficiency after optimization: (a) 15 July; (b) 22 July; (c) 30 July

is operated at full load. However, the CC net efficiency will decrease when the CC net load reaches about 45 % due to the follower GT start-up process (about 25 minutes).

During an interval of 45 minutes after the follower GT is already on (or 70 minutes since the start-up of the follower GT), the ST load has not been able to respond to changes in the load on the follower GT because the follower HRSG is still in the start-up process. After the start-up processes of both follower GT and follower HRSG are completed in 71 minutes (calculated from the start-up of follower GT), the load changes on both GT can be immediately responded by ST.

Figure 18 shows the actual part-load efficiency of the CCPP with the lowest and highest load ranges (based on data collected as of July 2019) after the optimization. The graph shows the highest performance that the CCPP can achieve, wherever the load is. A higher CC net efficiency means the power plant consumes less fuel to generate the same

power. The decrease in fuel consumption after the optimization can be seen in Figure 19.

F. Energy and cost saving of load optimization

Table 5 shows the total energy saving obtained from the three optimization time ranges according to the simulation results. This energy saving has MMBTU unit, with a total of 1,146.09 MMBTU during July 2019. Table 6 shows the total cost saving obtained by multiplying the energy saving (in MMBTU) by the price of the fuel (in \$/MMBTU). This natural gas fuel is supplied by three vendors with different usage ratios and prices. Therefore, cost saving will be calculated based on these parameters.

Table 7 shows the total cost savings of fuel consumption from this load optimization, which is IDR 152,249,551.76, or 5.24 % of the cost during the observation data (July 2019). It should be noted that any loading error in a large capacity power plant will result in greater losses when compared to a smaller capacity power plant.

G. Load optimization feasibility analysis

From a technical point of view namely equipment safety, there are no constraints because all equipments are operated in the design operation range (0 - 100 %) so there are no overloads and losses outside of the routine O&M can be avoided. In addition, observations of GT start-up and shutdown in July 2019 were well monitored. Start-up and shutdown of GT1 and GT2 were done alternately,

thus minimizing damage to one GT because it was operated continuously as the main GT.

From an economic point of view, there are no constraints because this optimization does not require investment. This happens because the optimization carried out is in the form of a more optimal operation management. All equipment performances are also still high considering its very new age.

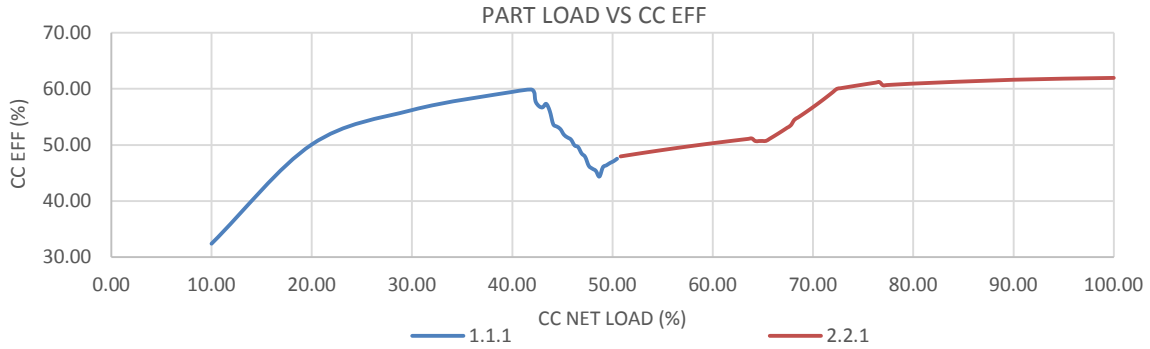


Figure 18. Actual CC net efficiency after optimization

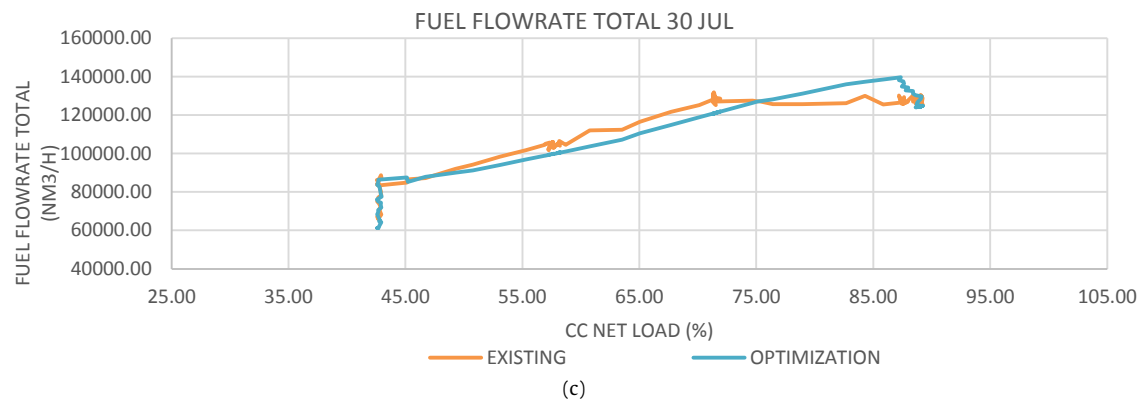
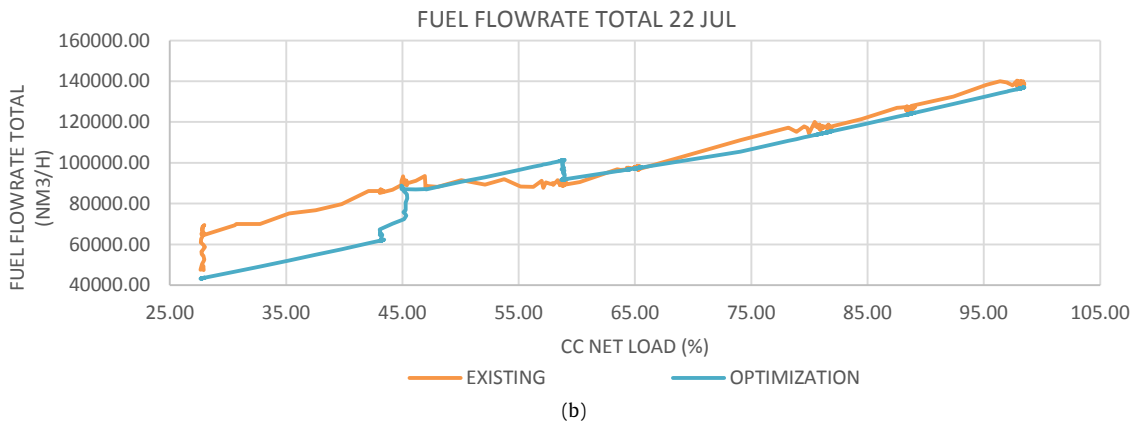
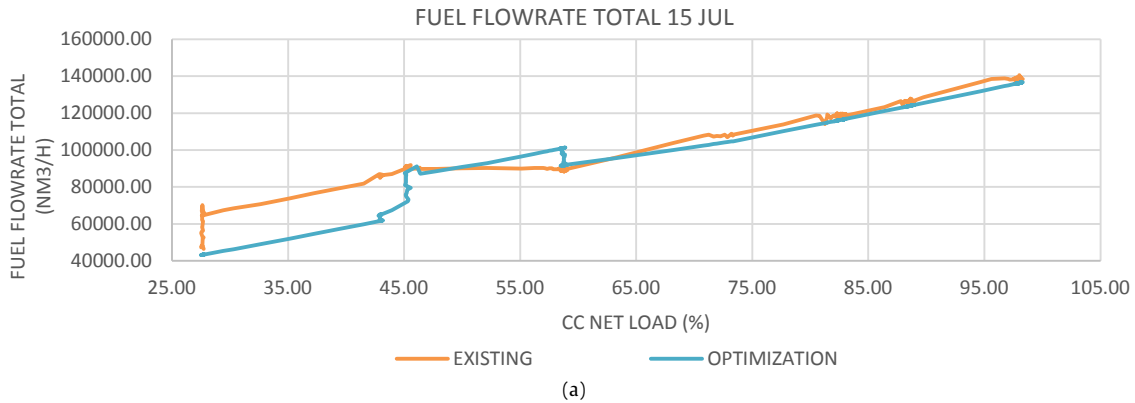


Figure 19. Fuel flowrate after optimization: (a) 15 July; (b) 22 July; (c) 30 July

Table 5.
Energy saving after load optimization

Optimization range	Energy saving (MMBTU)
15/07/2019 04:27:00 to 11:34:00	450.06
22/07/2019 02:58:00 to 11:31:00	510.92
30/07/2019 09:53:00 to 11:52:00	185.11
Total	1,146.09

Table 6.
Natural gas use and price July 2019

Fuel vendor	Ratio	Price (\$/MMBTU)	\$ exchange rate (IDR)
PT PGN Tbk	15.83	7.97	
PT Nusantara Regas	22.49	10.62	13,956.00
BP Berau Ltd.	1	9.35	

Table 7.
Cost saving after load optimization

Description	Unit	Value
Fuel saving	MMBTU	1,146.09
PT PGN Tbk	\$	3,677.46
PT Nusantara Regas	\$	6,959.34
BP Berau Ltd.	\$	272.46
	\$	10,909.25
Total	IDR	152,249,551.76
	% cost	5.24

IV. Conclusion

This journal has discussed the loading of CCPP Block 4 (Jawa-2) at PT Indonesia Power Priok POMU during July 2019; with the discovery of three conditions with the use of 2.2.1 (2 GT, 2 HRSG, 1 ST) configuration in CC net load of about 30 - 45 %, which in fact could be compensated by 1.1.1 (1 GT, 1 HRSG, 1 ST) configuration. These conditions resulted in the CC net load performance was being lower than its baseline. Then the loading configuration was optimized, by changing the configuration from 2.2. 1 to 1.1.1 (or by activating only one GT) for the 0 - 50 % of CC net load through simulations. The result was that the CC net load performance after the optimization increased, with energy saving of 1,146.09 MMBTU or equivalent to cost saving of IDR 152,249,551.76.

Acknowledgment

The authors would like to thank PT Indonesia Power Priok POMU, especially our gratitude to Mr. Suparlan, Mr. Rahmat Santoso, and Mr. Alief Rakhman Mukhtar for the internship opportunity at the company and providing all the operational data.

Declaration

Author contribution

Louise Indah Utami is the main contributor of this paper. All authors read and approved the final paper.

Funding statement

This research did not receive any specific grant from funding agencies in the public, commercial, or not-for-profit sectors.

Competing interest

The authors declare that they have no known competing financial interests or personal relationships that could have appeared to influence the work reported in this paper.

Additional information

Reprints and permission: information is available at <https://mev.lipi.go.id/>.

Publisher's Note: National Research and Innovation Agency (BRIN) remains neutral with regard to jurisdictional claims in published maps and institutional affiliations.

References

- [1] G. Khankari and S. Karmakar, "4-E analysis of a Kalina cycle system 11 integrated 500MWe combined thermal power plant," *TENCON 2017 - 2017 IEEE Region 10 Conference*, pp. 93-98, 2017.
- [2] Mohammad Ali Motamed and Lars O. Nord, "Assessment of organic Rankine cycle part-load performance as gas turbine bottoming cycle with variable area nozzle turbine technology," *MDPI Energies Journal*, vol. 14, 2021.
- [3] V. S. Kuz'michev, A. Y. Tkachenko, Y. A. Ostapyuk, I. N. Krupenich and E. P. Filinov, "Features of computer modeling of the working process of small-scale gas turbine engines," *2017 International Conference on Mechanical, System and Control Engineering (ICMSC)*, pp. 136-140, 2017.
- [4] Dan-Teodor Balanescu and Vlad-Mario Homutescu, "Performance analysis of a gas turbine combined cycle power plant with waste heat recovery in organic Rankine cycle," *Procedia Manufacturing (The 12th International Conference Interdisciplinarity in Engineering)*, vol. 32, pp. 520-528, 2019.
- [5] M. J. B. Kabeyi and O. A. Olanrewaju, "Performance analysis of an open cycle gas turbine power plant in grid electricity generation," *2020 IEEE International Conference on Industrial Engineering and Engineering Management (IEEM)*, pp. 524-529, 2020.
- [6] Yongyi Li, Guoqiang Zhang, Ligang Wang, and Yongping Yang, "Part-load performance analysis of a combined cycle with intermediate recuperated gas turbine," *Energy Conversion and Management*, vol. 205, 2020.
- [7] Dede Mavendra, "Kalkulasi efisiensi daya mesin plgtu dengan pola operasi 2-2-1 dan 3-3-1 PT Indonesia Power Unit Pembangkitan Semarang," *USD Repository*, 2016.
- [8] Xiang Wan, Niansu Hu, Pengfei Han, Shiqi Li, "Performance monitoring of the gas-steam combined cycle unit in multi-energy power grid," *Proceedings of the 2015 International Conference on Sustainable Energy and Environmental Engineering*, Oct. 2015.
- [9] Michael Welch, "Improving the Flexibility and Efficiency of Gas Turbine-Based Distributed Power Plant," *8th International Gas Turbine Conference, ETN Global*, 2016.
- [10] Vicky, Wegie Ruslan, and Anthony Riman, "Optimization of combined-cycle power plant operating pattern," *RIP International Journal of Applied Engineering Research*, vol. 12, no. 21, pp. 11576-11582, 2017.
- [11] Wartsila, *Combustion engine vs gas turbine: part load efficiency and flexibility*. Wartsila, 2022.
- [12] Yunus A. Cengel and Michael A. Boles, *Thermodynamics: an engineering approach*. US: McGraw Hill, 5th ed, p. 584, 2004.
- [13] V. Camacho and R. Chaer, "Hourly model of a combined cycle power plant for SimSEE," *2020 IEEE PES Transmission & Distribution Conference and Exhibition - Latin America (T&D LA)*, pp. 1-5, 2020.
- [14] Mitsubishi Power, *GTCC gas turbine combined cycle power plants*. mitsubishi power, 2021.
- [15] M. Olga, C. Pavel and P. Andrey, "Combined cycle power plant control during frequency excursions," *2017 9th International Conference on Information Technology and Electrical Engineering (ICITEE)*, 2017, pp. 1-5, 2017.